Renewable Energy 218 (2023) 119263

Contents lists available at ScienceDirect

Renewable Energy

journal homepage: www.elsevier.com/locate/renene

Building envelope-enhanced phase change material and night ventilation: Effect of window orientation and window-to-wall ratio on indoor temperature

Qudama Al-Yasiri [a,b,c,*], Mohammed Alktranee [d], Márta Szabó [b], Müslüm Arıcı [e]

[a] Doctoral School of Mechanical Engineering, MATE, Szent István Campus, Páter K. U. 1, Gödöllő, H-2100, Hungary
[b] Department of Building Engineering and Energetics, Institute of Technology, MATE, Szent István Campus, Páter K. U. 1, Gödöllő, H-2100, Hungary
[c] Department of Mechanical Engineering, Faculty of Engineering, University of Misan, Al Amarah City, Maysan Province, 62001, Iraq
[d] Department of Mechanical Techniques, Technical Institute of Basra, Southern Technical University, Basrah, Iraq
[e] Department of Mechanical Engineering, Faculty of Engineering, Kocaeli University, Umuttepe Campus, Kocaeli, 41001, Turkey

ARTICLE INFO

Keywords:
Phase change material
Window-to-wall ratio
Window orientation
Night ventilation
Indoor temperature reduction
Thermal comfort

ABSTRACT

Integrating phase change material (PCM) and natural night ventilation (NNV) has notably improved building indoor thermal comfort in hot locations. The current study investigates the role of NNV through a window to improve the indoor temperature of a PCM room, considering the window orientation and window-to-wall ratio (WWR). The NNV was employed through a one-sided window of the PCM room to enumerate the advantages of passive building technologies in summer. Different window orientations and WWRs (between 8.75% and 20%) were analysed to improve the indoor environment using an experimentally validated model developed by EnergyPlus software. Numerical findings exhibited that the window orientation has a minimal effect on the NNV of the PCM room regardless of wind direction. However, the Northeast orientation was the best case for the studied location, achieving average indoor temperature reduction by up to 31%, and a thermal load levelling reduction by 9%–17%. Furthermore, the larger window size exhibited improved thermal comfort, where the WWR of 20% decreased the average indoor temperature by 1.14 °C more than the reference PCM room of WWR = 8.75% without ventilation. Besides, the operative temperature at the largest window size was reduced by up to 22% during nighttime. The study concluded that the effectiveness of NNV is limited under severe hot locations, and alternative cooling means could be advantageous.

1. Introduction

The energy share in the building sector is drastically increasing year after year, reaching alarming levels due to fast urbanisation, population and increased lifestyle requirements [1]. The UN Environment Program stated in the latest released report in 2022 that building energy consumption and CO_2 emissions are increased compared with the 2021 status regardless of the substantial investment on global levels [2]. In this regard, it has been quantified that the energy demand and CO_2 emissions augmented by 4% and 5%, respectively, compared with the status of 2020, indicating the biggest increase in the last ten years [2]. As stated by the Intergovernmental Panel on Climate Change, the energy consumption on cooling and heating in residential and commercial buildings is increasing globally, reaching 183% and 179%, respectively, by 2050, compared to 2010 [3].

Engineers and architects are working to increase the thermal comfort standards in modern buildings since occupants spend 80%–90% of their daily hours indoors [4]. To this aim, different passive/active strategies are proposed to maintain a better-built environment, implemented in the building design phase or added in the later phases of construction [5]. Numerous studies indicated that building envelope advancements are more remarkable in saving energy and maintaining better indoor thermal comfort [6], especially those associated with building morphology [7]. For building retrofitting and energy management possibilities, phase change materials (PCMs) have been announced as essential strategies to reduce buildings' heating and cooling demand [8, 9]. PCMs are unique materials able to store vast extent of heat energy within a limited volume and discharge it when desired. This exceptional property allowed it to be utilised in different energy-related

* Corresponding author. Doctoral School of Mechanical Engineering, MATE, Szent István Campus, Páter K. U. 1, Gödöllő, H-2100, Hungary.
E-mail addresses: qudamaalyasiri@uomisan.edu.iq (Q. Al-Yasiri), mohammed.hr@stu.edu.iq (M. Alktranee), szabo.marta@uni-mate.hu (M. Szabó), muslumarici@gmail.com (M. Arıcı).

https://doi.org/10.1016/j.renene.2023.119263
Received 1 May 2023; Received in revised form 28 August 2023; Accepted 2 September 2023
Available online 2 September 2023

Nomenclature

Abbreviations

$A_{opening}$	The opening area (window area) [m^2]
ACH	Air change per hour
AITR	Average indoor temperature reduction [%]
CondFD	Conduction finite difference algorithm
C_w	Opening effectiveness
EA	Effective angle [°]
EPW	EnergyPlus weather file
$F_{schedule}$	The fraction of opened window (ranging from 0% to 100%)
IDF	Information data file
NNV	Natural night ventilation
NV	Night ventilation
OTR	Operative temperature reduction [%]
OT	Operative temperature [°C]
PCM	Phase change material
Q_w	Volume of air flow rate driven by wind [m^3/s]
TLL	Thermal load levelling
TLLR	Thermal load levelling reduction [%]
WD	Wind direction

Symbols

c_p	Specific heat of layer [kJ/kgK]
H_f	Heat of fusion [kJ/kg]
h	Specific enthalpy of layer [kJ/kg]
h_i	Combined heat transfer coefficient for the inner envelope [W/m^2K]
h_o	Combined heat transfer coefficient for the outer envelope [W/m^2K]
I_{inc}	Solar radiation on inclined surface [W/m^2]
i	Node under modelling
i+1	*Nearby node as to indoor side*
i-1	*Nearby node as to outdoor side*
j+1	Instantaneous time-step
k	The thermal conductivity of layer [W/m.K]
k_E	The thermal conductivity for the edge between i and i-1 nodes [W/m.K]
k_W	The thermal conductivity for the edge between i and i+1 nodes [W/m.K]
T	The temperature of a node under modelling [K]
T_i	The indoor temperature [K]
$T_{sol\text{-}air}$	Solar-air temperature [K]
$\overline{T_{mr}}$	The mean radiant temperature [K]
ΔR	The difference between long-wave radiation incident on the surface (from the sky) and radiation emitted by the blackbody [Unitless]
Δt	The time-step [s]
Δx	The layer thickness [m]

Greek symbols

α	Absorptivity coefficient [Unitless]
β	Hemispherical emittance of outside element surface [Unitless]
ρ	Density [kg/m^3]

applications, including buildings, for thermal energy management and energy storage [10,11]. Market reports expect an increment in the PCM market by up to 889 million USD in 2025, compared with 423 million USD in 2020 due to notable PCM advantages [12].

Considering building cooling demand, combining PCMs and night ventilation has recently proven to be a remarkable improvement, particularly in mild locations [13]. Night ventilation (NV) is employed actively or passively to improve the building environment and save energy effectively. In active NV applications, air velocity plays a core role in accelerating heat removal from PCM elements and improving indoor thermal comfort. Furthermore, wind speed is the foremost influencer of PCM utilisation in NNV studies [14]. However, PCM charging and discharging phases could be improved along with notably reduced time [15]. Recent literature studies have been extensively dedicated to investigate the combined effect of PCM and NV on improving the indoor environment and augmenting energy-saving. Commonly studied topics were PCM characteristics (PCM transition temperature and quantity at most), NV time, ventilation flow rate and speed, ventilation temperature, etc. In addition, most of these studies have reported maximised benefits for the built environment due to improved thermal storage potential of PCM during negative behaviour at nighttime. These studies are generally conducted under moderate weather conditions, where the NV could work effectively alone without requiring PCM incorporation [16]. Besides, mechanical NV was extensively investigated due to its superior thermal benefits compared with natural NV, although it has technical and economic concerns [17].

Given the combined effect of PCM-enhanced building envelopes and NV in the recently published research work, Kitagawa et al. [18] numerically explored the effect of NV on a PCM-enhanced floor cooling system under hot location. The study considered the natural and forced NV operation schedule, ventilation flow rate, effective underfloor height space, and thickness of the PCM layer as effective parameters. The findings showed that the optimal schedule for fan operation was from 19:00 to 7:00 in hot and humid locations. Moreover, the ventilation flow rate speed was the most effective key parameter, in which 700 CFM (cubic feet per minute) was sufficient, and the NV with 6 mm PCM thickness was optimal for the proposed cooling system. Rangel et al. [19] experimentally researched the effect of naturally ventilated PCM roofs to quantify a test module's indoor air temperature reduction, time lag, and solidification time extension. The study results disclosed a maximum indoor temperature decrease by 3.94%–7.02%, a peak time lag of about 10–70 min, and a PCM solidification time extension of 19%–41%. Liu et al. [20] investigated the role of PCM-integrated building envelope coupled with NNV to enhance the thermal comfort inside buildings in ten Chinese cities. The EnergyPlus tool was adopted to investigate melting temperatures varying from 23 °C to 29 °C, the optimal for studied locations. As a general conclusion, the study found that discomfort hours decreased by at least 16% in all cities when the PCM/NNV was adopted compared with the use of NV alone. Yu et al. [21] numerically studied the heat gain reduction for a ventilated pipe-embedded PCM roof under climate conditions of different Chines regions. The results generally showed that coupling PCM with ventilation is necessary to utilise PCM heat storage, and the optimal PCM transition temperature varies in each region. However, the heat gain decreased by 300.67 kJ/m^2 in all studied locations. Luo et al. [22] numerically explored the heat flux reduction, interior surface temperature fluctuation reduction, and the frequency of thermal discomfort for a porous brick roof ventilated naturally under different Cities in China. At the best PCM melting temperature, the study revealed that the roof reduced heat flux by up to 95.2 kJ/m2 and minimised thermal comfort frequency by up to 37.2%. Aamodt et al. [23] experimentally investigated the role of NV in overcoming the passive PCM heat storage behaviour when installed into ventilated ceiling and walls of an office module in Oslo, Norway. They studied the cooling load reduction and energy saving under different airflow rates (0.5–5 air changes per hour (ACH)) and PCM thicknesses (2–4 mm). Study findings showed that the building cooling load was reduced by 19.5%, 78.2% and 95.5% at 4 mm PCM thickness employed with 1, 3 and 5 ACH, respectively. The natural

NV helped to save energy by 56% at 3 ACH and by 69% when 4 mm PCM thickness was employed. Besides, the hybrid NV showed energy saving by 38% at the same flow rate and augmented to 50% at 4 mm PCM thickness. Prabhakar et al. [24] studied the energy efficiency of PCM walls, partitions and a ceiling integrated with a controlled ventilation system. The PCM/NV effectiveness for cooling application was quantified under controlled/non-controlled mode. The study findings revealed that PCM effectiveness improved from 3.3% to 25.6% by combining PCM with NNV and increased to 40% with the temperature-controlled ventilation mode. Hou et al. [25] experimentally studied the thermal performance of a room-integrated multiple PCM ventilated roof compared with another priston one without PCM. The study calculated the indoor air temperature reduction and thermal dissatisfaction rate while applying natural and forced NV. The findings showed that the peak indoor air temperature was reduced by 41.1%–44.9% using NNV, while it was reduced by 43.2%–47.0% under forced NV. Besides, the study concluded that the thermal dissatisfaction rate was reduced by 15.5% and 40.2% under natural and forced NV, respectively. In a similar approach, Fan et al. [26] have studied the heat flow reduction, interior surface temperature difference, and attenuation coefficient of a test room-integrated PCM-ventilated wall. The outcomes showed that the modified PCM wall had reduced the maximum heat flow by 78.5% and the interior temperature by up to 7.4 °C. moreover, the attenuation coefficient was reduced by 13.5%–25.7%, employing forced NV and PCM. Zavrl et al. [27] have experimented two units in which PCM plates-integrated roof and internal wall with air gap were proposed in one unit and the other left for comparison. The study analysed the indoor air temperature reduction and optimal PCM solidification requirements during the night period. The indoor temperature was reduced by up to 5 °C. Study outcomes indicated that the optimal PCM solidification was attained using the developed ventilated air-gap system with 15 °C–16 °C ventilation air temperatures and 500 m^3/h flow rate. Ji et al. [28] proposed a PCM wallboard-attached NV system to enhance a room module's indoor temperature and thermal comfort time in Chongqing, China. According to the study outcomes, the indoor air temperature and west-wall surface temperature were decreased by 94.97% and 67.74%, respectively. Besides, the time of thermal comfort was extended by 38.42%. Under Danish weather conditions, Hu et al. [29] studied the annual energy saving of a PCM window with various control strategies. The control strategy proposed for the summer night cooling indicated cooling demand reduction by up to 62.3% compared with the primitive control strategies with NNV. Adopting a different approach, Hu et al. [30] numerically investigated the energy-saving potential of a PCM window for a sustainable house in New York City under a controlled ventilation airflow rate. In the best scenario, the proposed system indicated building energy saving by 12% at a 300 m^3/h airflow rate compared with a standard window. Furthermore, the adopted strategy has enhanced the house energy saving by 14.7% over the constant ventilation airflow rate.

Based on the above literature studies, the combination of PCM with NV has notable benefits in enhancing building energy and maintaining indoor thermal comfort under various building applications. However, there is still a research gap for other PCM incorporation interactions with the passive architectural building aspects. Besides, most studies considered the mechanical NV, which has technical complexity and economic concerns for long-term building service. Hence, this study was conducted to investigate the role of NNV in improving the indoor environment of building envelope integrated with PCM under hot summer considering the window orientation and WWR. The influence of NNV on indoor thermal comfort under different window orientations is studied in terms of the reduction of indoor temperature and thermal load levelling. Besides, the WWR was analysed for different window sizes at the best window orientation, considering the reduction of indoor and operative temperatures. This study is believed to enrich the knowledge with passive booming technologies in the building industry under harsh weather conditions.

2. Research methodology and modelling

The flowchart of this research is presented in Fig. 1. Each phase of the methodology was conducted to be the input to the next phase. More description of phases is detailed in the following subsections.

2.1. Physical model

A separate room of 1000 mm^3 was modelled using the Google SketchUp tool, identical to the experimental room presented in our earlier study [31]. The numerical simulation was confirmed for six consecutive months, from May–October 2021, the summer months of Al Amarah City, Iraq. The room had a composite flat roof comprised of three main layers: Isogam roofing, concrete, and gypsum mortar cladding. Besides, the room walls were built from concrete bricks covered with a thin cement mortar layer from the outside. The room was oriented towards the east, in which the east-oriented wall included a small window of 250 × 350 mm dimensions (WWR of 8.75%). The floor was assumed insulated using a woody foundation with 50 mm thickness. The room was incorporated with an organic PCM within the roof and walls. The PCM with 15 mm thickness was included in the roof between the roofing and concrete layer, while a 7 mm of the same PCM type was incorporated in the middle of brick walls. The PCM employed in this study is a paraffin wax, a petroleum-based product extracted in the course of the de-waxing of the Iraqi crude oil. This PCM type was selected due to its adequate thermal properties, including a transition temperature of about 40 °C–44 °C suitable for the study location and high latent heat of fusion (around 1900 kJ/kg), not to mention its economic competence [32]. The PCM layer position in the roof and the thickness included in the roof and walls were considered according to the earlier follow-up preliminarily studies [33–35]. Fig. 2 shows the PCM room model described above, and Table 1 shows the thermal and physical features of the PCM and construction materials.

2.2. Simulation tool and procedure

The simulation of the PCM room model was conducted by the EnergyPlus tool, which was established by DOE-USA and broadly implemented for building dynamic energy simulations. The EnergyPlus employs editable information data file and weather file to specify the construction materials, simulation methodologies, weather information, and many other inputs and advanced control aspects. The software was provided with the ability to simulate the PCM-based buildings through a one-dimensional conduction finite difference algorithm (CondFD) that can easily solve the phase transition phenomenon along with the construction materials. Accordingly, the PCM layers involved in the PCM room model were mathematically conveyed using a fully-implicit first-order scheme. The model equation of this scheme is based on the Adams-Moulton solution specified in Eq. (1) as follows:

$$\rho C_p \Delta x \frac{T_i^{j+1} - T_i^j}{\Delta t} = \left(k_W \frac{\left(T_{i+1}^{j+1} - T_i^{j+1}\right)}{\Delta x} + k_E \frac{\left(T_{i-1}^{j+1} - T_i^{j+1}\right)}{\Delta x} \right) \quad (1)$$

A time-step test (Δt) was conducted, and $\Delta t = 3$ min (20 times/h) *was considered in the present study. This time-step is suitable* to simulate the phase transition phenomenon by EnergyPlus, as *recommended by* Tabares-Velasco et al. [38] and others [39–41]. The thermal conductivities k_W and k_E are determined using Eqs. (2) and (3), as follows:

$$kw = \frac{\left(k_{i+1}^{j+1} + k_i^{j+1}\right)}{2} \quad (2)$$

$$k_E = \frac{\left(k_{i-1}^{j+1} + k_i^{j+1}\right)}{2} \quad (3)$$

The C_p of each PCM node is updated in each iteration scheme of the CondFD, resulting in variable Cp, written by Eq. (4) as follows:

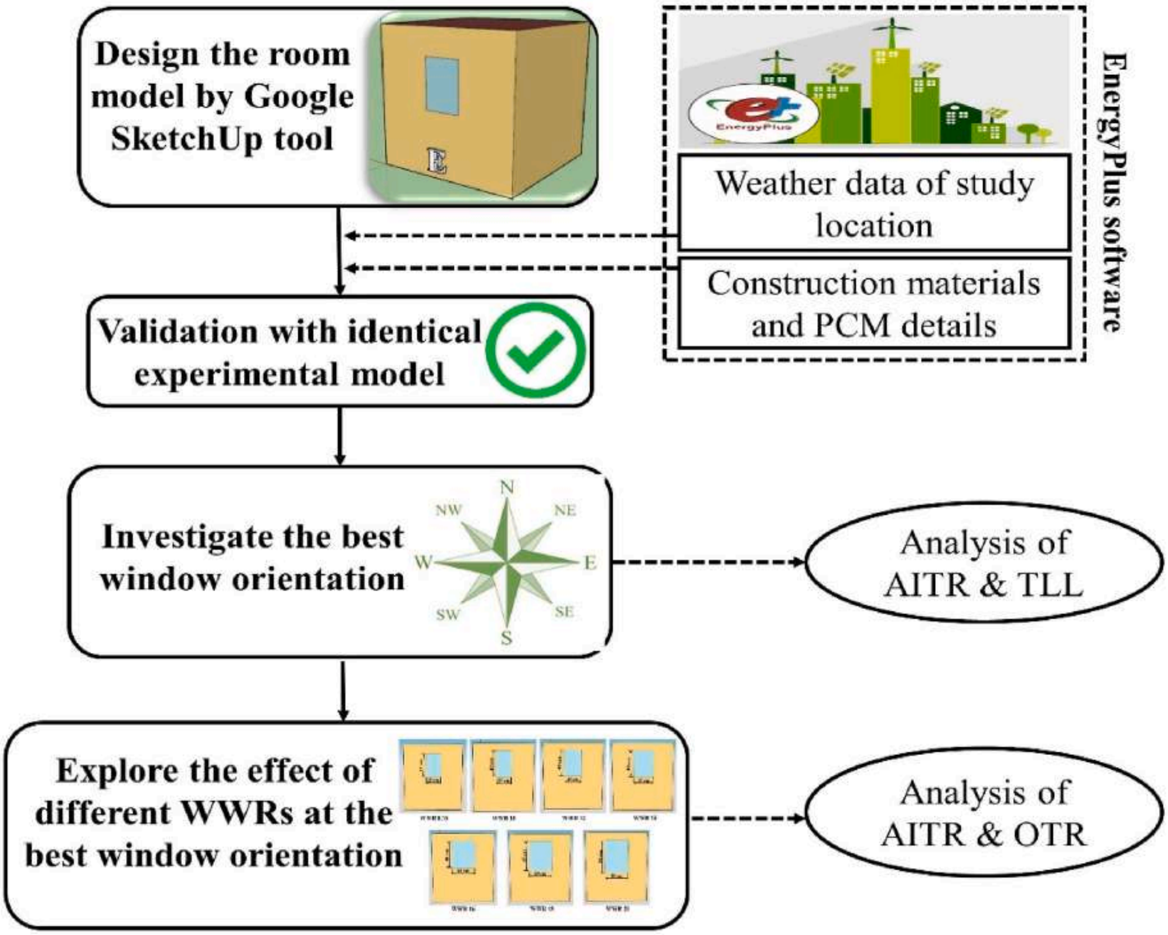

Fig. 1. Flowchart of research methodology.

$$C_p = \frac{h_i^j - h_i^{j-1}}{T_i^j - T_i^{j-1}} \tag{4}$$

The PCM-specific enthalpy h (in kJ/kg) is specified as a temperature-dependent value, according to Eq. (5) [42].

$$h = h(T) \tag{5}$$

The main assumptions considered in the simulation to simplify the transient heat transfer model by the CondFD algorithm are as follows:

- All materials/layers are assumed isotropic and homogeneous, and no heat is generated within each material/layer.
- The PCM layer is perfectly contacted with the construction materials, so the contact resistance is insignificant.
- No hysteresis occurs within the PCM during the melting and solidification phases.
- The so-called sol-air temperature ($T_{sol-air}$) is presented to quantify the elements' outer surface temperature, considering the outdoor air temperature (T_a), inclined solar radiation (I_{inc}), outdoor convection heat transfer (h_o), and the absorptivity coefficient of the element (α), according to Eq. (6) [43].

$$T_{sol-air} = T_a + \frac{\alpha I_{inc}}{h_o} - \frac{\beta \Delta R}{h_o} \tag{6}$$

The term $\frac{\beta \Delta R}{h_o}$ was assumed equal to 3.9 °C and 0 °C, respectively, for the horizontal and vertical surfaces [44].

Since the current work focuses on the NNV, the whole ventilation process is controlled by the wind, according to Eq. (7) [45], as follows:

$$NNV = Q_w \; C_w A_{\text{opening}} F_{\text{schedule}} V \tag{7}$$

The $F_{schedule}$ fraction of open area is defined in the EnergyPlus schedule as 0 and 1, in which 0 means closed window and 1 refers to 100% open window. Besides, C_w is obtained for each time-step considering the angle between the wind direction and effective angle, according to Eq. (8), as follows:

$$C_w = 0.55 - \frac{|\text{EA} - \text{WD}|}{180} * 0.25 \tag{8}$$

The EA and WD difference should range between 0° and 180°, and in case it is more than 180°, the difference is reset to −180° degrees. This formulation is a linear interpolation using the recommended values by the 2009 ASHRAE Handbook- Fundamentals (0.5–0.6 for perpendicular wind directions and 0.25–0.35 for diagonal directions).

2.3. Model validation

Many research works have been implemented to verify the numerical models of building-related applications simulated using the EnergyPlus tool compared to experimental/numerical studies [46,47]. The developed numerical model in this work has been validated against our earlier experimental data obtained for a room built from the same construction materials and examined under similar climate conditions on 23 September 2021 [31]. Since enhancing indoor temperature is the core of this work, the numerical and experimental data were compared concerning the improvement in indoor temperature of the PCM rooms with/without modification. The validation showed good agreement between the numerical and experimental data, with an acceptable

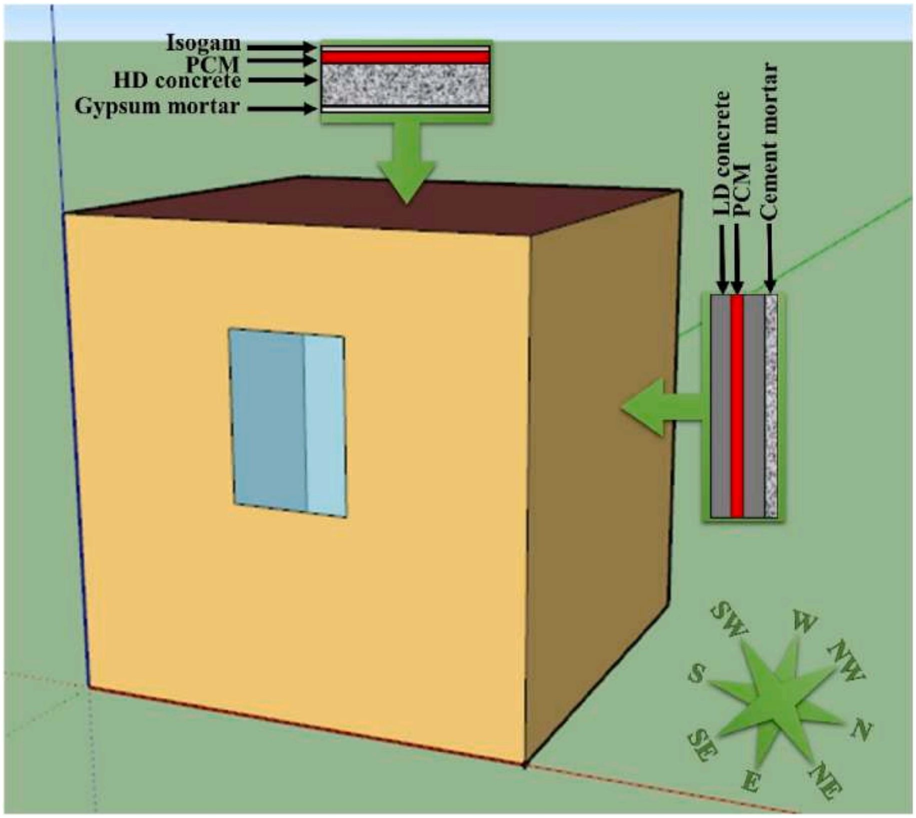

Fig. 2. Physical model of PCM room.

Table 1
Characteristics of construction materials/elements [36,37].

Construction element	Layer thickness (cm)	k (W/m.K)	ρ (kg/m^3)	C_p (J/kg.K)
Isogam	0.4	0.35	1400	1100
Concrete	5	1.49	2300	800
Gypsum mortar	0.2	0.23	980	896
Cement mortar	1–2	0.99	2020	1000
Concrete brick	7	1.4	1440	750
PCM	1.5 (roof)	0.48 (solid)	830 (solid)	2210 (solid)
	0.7 (wall)	0.22 (liquid)	878 (liquid)	2300 (liquid)
Plywood	3	0.18	950	1200
Single glazing pane	0.6	–	–	–

deviation of a maximum of 4.3% and 3.5% between the reference and PCM room indoor temperatures, respectively (Fig. 3). This deviation of findings could be attributed mainly to the difference between the actual weather conditions measured on-site and the predicted weather data delivered in the simulation EPW file. Furthermore, the thermal characteristics of construction layers involved in the simulation IDF file were not accurately similar to those of the experimental room as they were taken from the typical construction blog [36]. Moreover, the CondFD algorithm did not consider the thin encapsulation layer, which is necessary in the experimental study to avoid PCM leakage, causing a slight difference between the numerical and experimental outputs.

2.4. Evaluation of indoor improvement

The influence of natural night ventilation (NNV) was investigated, considering the role of low ambient temperature at night to enhance the PCM room indoor temperature and improve its negative behaviour during the heat discharging phase. For this purpose, the numerical model was applied for two scenarios to show the influence of window orientation and window-to-wall ratio (WWR) on the PCM room indoor thermal comfort. These methods could help to highlight possible further enhancements in the indoor temperature that could be reached along with the PCM incorporation.

In the first scenario, the window orientation towards the east direction (E) was assumed as the reference case following the design specifications of the reference study [31]. The other orientations considered in the numerical simulation were the South (S), Southeast (SE), Southwest (SW), West (W), North (N), Northeast (NE), and Northwest (NW).

In the second scenario, the best building orientation obtained in the first scenario was adopted to explore the effect of WWR varied between 10% and 20% was investigated compared with the base case of WWR = 8.75%. Fig. 4 shows the proposed WWRs in this scenario.

Several parameters are used to evaluate the thermal comfort improvement in the current scenarios, including the average indoor temperature reduction, thermal load levelling reduction, and operative temperature reduction.

The average indoor temperature reduction (AITR) is the average decrease in the indoor temperature of the modified PCM room with NNV compared to the PCM room without NNV. This indicator was calculated in both studied scenarios (i.e., the effect of window orientation and varied WWRs). Mathematically, the AITR for the PCM room with NNV compared with the one without NNV in both scenarios was calculated according to Eq. (9).

$$AITR = \frac{T_{i,without\ NNV} - T_{i,with\ NNV}}{T_{i,without\ NNV}} \times 100\% \tag{9}$$

The thermal load levelling index (TLL) quantifies the fluctuations inside the built environment throughout the day cycle concerning the indoor maximum and minimum temperatures. In view of that, the low

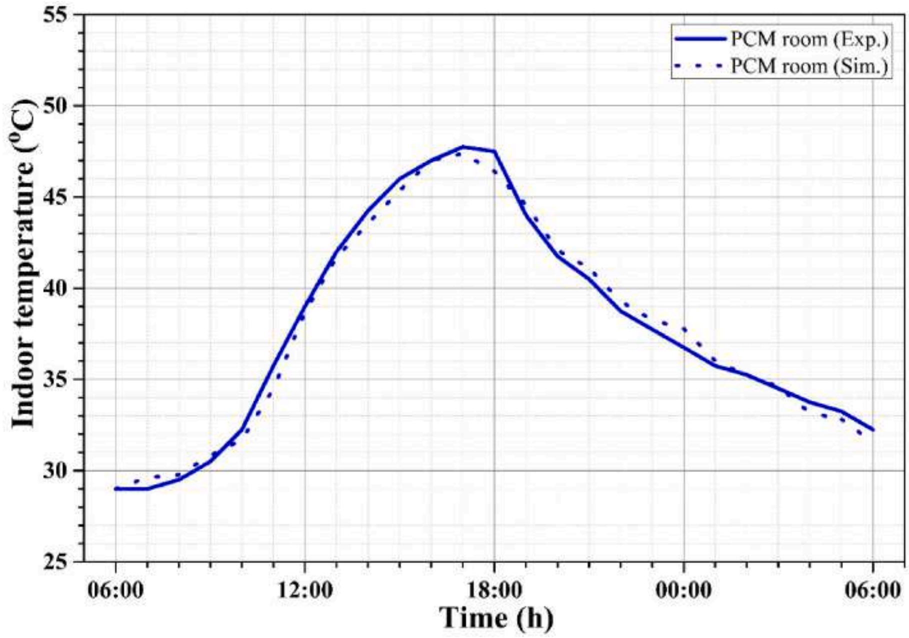

Fig. 3. Numerical model verification against experimental work [31].

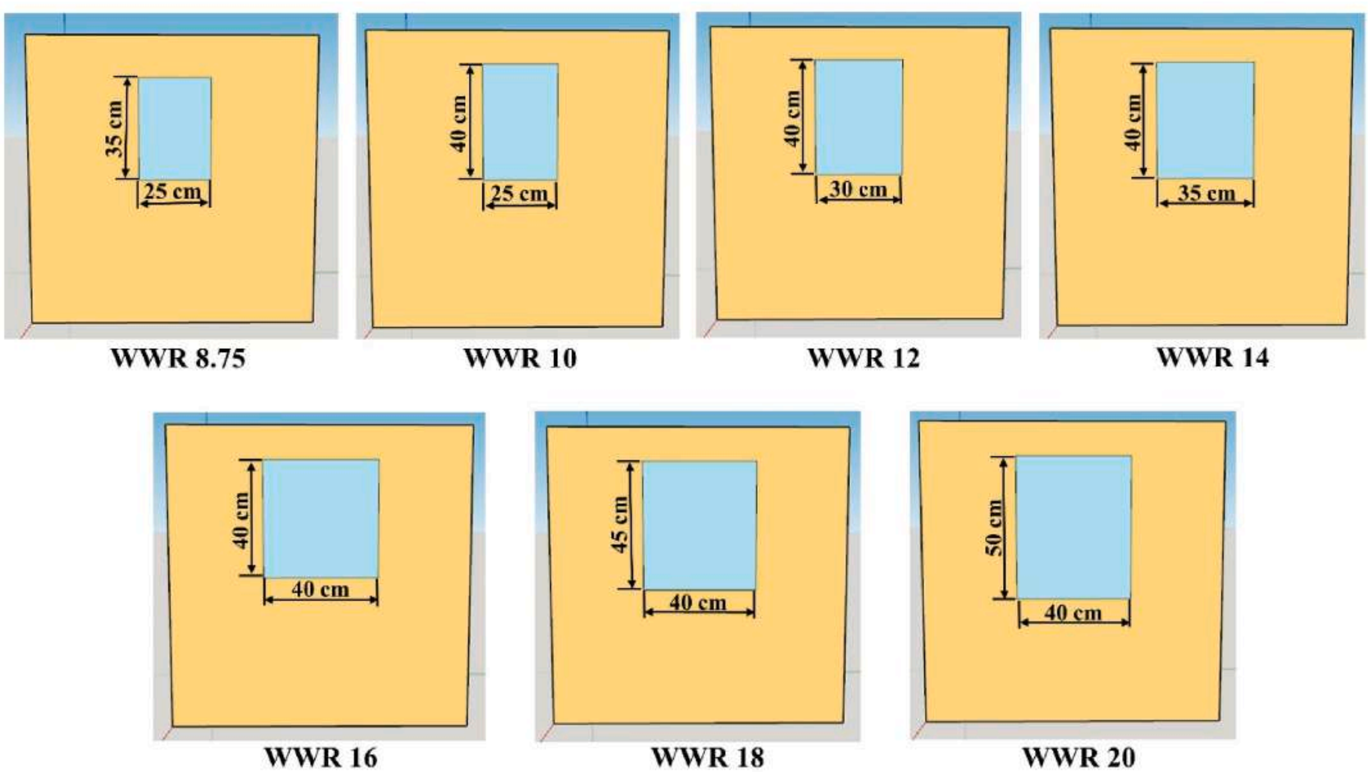

Fig. 4. Proposed WWRs.

TLL of a room designates improved thermal performance of its elements (i.e., building envelope) to minimise the fluctuation between the high and low temperatures. The TLL expression for a room was estimated using Eq. (10) [48], as follows:

$$TLL_{room} = \frac{T_{i,max} - T_{i,\ min}}{T_{i,max} + T_{i,\ min}} \quad (10)$$

The TLL reduction (termed as TLLR) is adopted in the first scenario of this work to compare the PCM room thermal performance under NNV and specific orientation against the one without NNV.

The operative temperature gives a powerful indication of thermal enhancement in the built environment since it is the temperature the occupants feel [49]. This indicator considers the average indoor air temperature and mean radiant temperature of interior building envelope surfaces, according to Eq. (11).

$$Operative\ temperature = \frac{T_i + \overline{T_{mr}}}{2} \tag{11}$$

where $\overline{T_{mr}}$ is the mean radiant temperature calculated each time step by the simulation tool. Subsequently, the OTR is quantified considering the average operative temperature of the PCM room-enhanced with NNV through the reference window (WWR = 8.75%), oriented towards the best window orientation, compared with the same room with vary WWRs (presented in Fig. 4). Mathematically, the OTR was calculated following the same representation to calculate the AITR (i.e., Eq. (9)).

3. Results and discussion

3.1. Location of study

The numerical simulation was verified for six summer months, from May to October 2021, under Al Amarah city weather conditions (Lat.: 31.84° N and Long.: 47.14° E, see Fig. 5), Iraq. The summer of this location is harsh and categorised as a desert according to Köppen-Geiger [50]. The ambient temperature is typically high during diurnal and night hours, surpassing 45 °C and 30 °C, respectively.

Fig. 6 shows the average outside air temperature and solar radiation on horizontal surfaces of the study location during July, the hottest day in summer. The outdoor air temperature and solar radiation rate are remarkable in the PCM simulation studies since they determine the outer surface temperatures of building elements and other heat transfer coefficients in the software tool.

The figure shows that the average ambient air temperature is above 45 °C during the daytime, typically exceeding 50 °C in some days, and above 30 °C in the nighttime. This is meaningful to enhance the building envelope thermal performance under such locations that rely worryingly on high-performance cooling machines to secure thermal comfort. The solar radiation is also high in the location under study, above 900 W/m^2 during most summer months. However, solar radiation is lower in October and the following autumn and winter months.

Although the outdoor air temperature and solar radiation are essential for the PCM melting phase (heat charging), the wind speed and wind direction remarkably affect the PCM solidification, especially in the current work since the heat dissipation occurred passively. Fig. 7 displays the wind speed and wind direction during the study period, as offered in the EPW file of the software.

Fig. 7 displays that the wind speed is mostly below 10 m/s during the summer. Besides, the wind often blows from W and NW directions, except in the second half of October, where the wind blows mostly from the NE, E and SE.

Fig. 5. Geographical position of study location within Iraq's map.

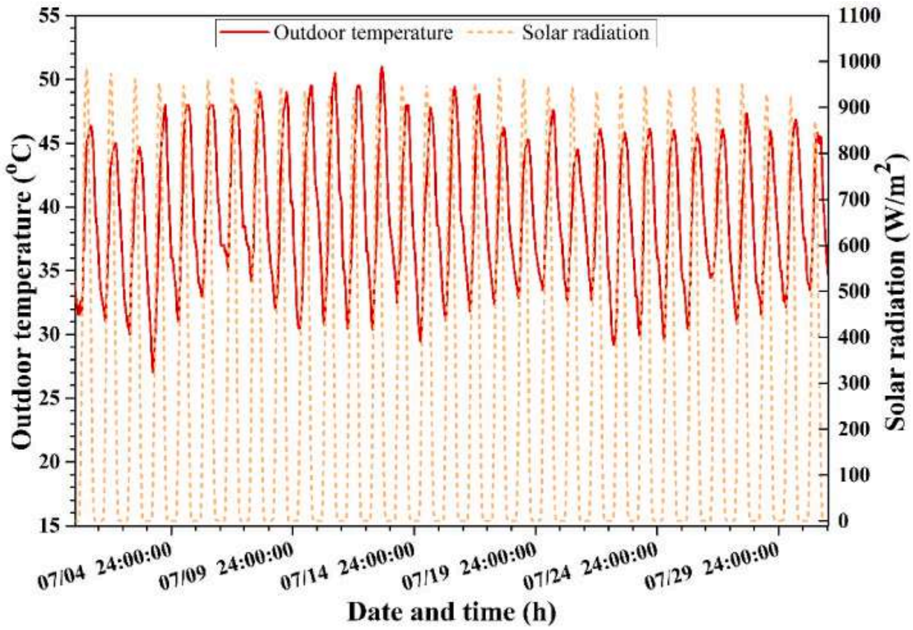

Fig. 6. Hourly outdoor air temperature and solar radiation.

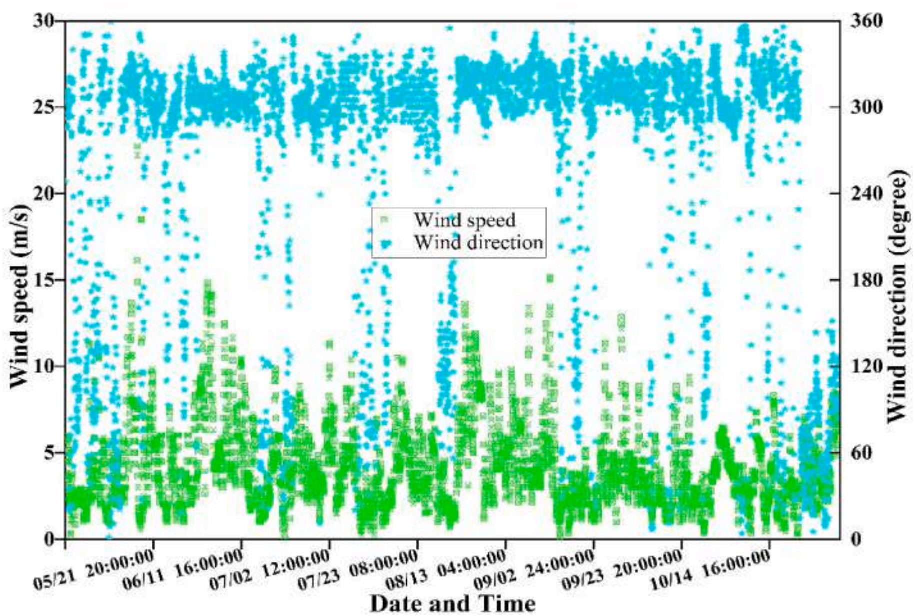

Fig. 7. Wind speed and direction from May to October.

Table 2
Maximum and minimum PCM room indoor temperature under NNV through different window directions.

		N	NE	E	SE	S	SW	W	NW
May	T_{max}	46.59	46.58	46.34	46.35	46.37	46.37	46.21	46.21
	T_{min}	37.59	37.54	37.42	37.47	37.50	37.48	37.33	37.31
Jun	T_{max}	50.19	50.19	49.89	49.89	50.04	50.04	49.65	49.65
	T_{min}	41.26	41.22	41.11	41.19	41.23	41.19	40.95	40.93
Jul	T_{max}	52.26	52.26	52.02	52.02	52.08	52.08	51.88	51.87
	T_{min}	42.99	42.97	42.91	42.96	42.97	42.94	42.81	42.80
Aug	T_{max}	52.32	52.31	51.96	51.96	51.87	51.87	51.84	51.84
	T_{min}	42.56	42.53	42.42	42.49	42.45	42.42	42.28	42.26
Sep	T_{max}	48.78	48.78	48.54	48.54	48.31	48.31	48.46	48.46
	T_{min}	39.42	39.40	39.25	39.28	39.20	39.17	39.23	39.19
Oct	T_{max}	41.05	41.05	40.73	40.73	40.59	40.59	40.99	40.98
	T_{min}	27.55	27.53	27.36	27.39	27.30	27.27	27.46	27.45

3.2. Effect of window orientation

The influence of window orientation on the PCM room under NNV was studied numerically compared with the reference case (E), considering the other three wall directions (i.e., S, W and N) for WWR of 8.75%. The other orientations are also studied by rotating the PCM room 45° clockwise (i.e., NE, SE, SW and NW). The daily NNV was applied for 6 h, from 18:00 to 24:00, over the simulation period of six summer months. The average maximum and minimum PCM room indoor temperature with NNV considering all orientations, are listed in Table 2. The table displayed remarkable temperature disparity between the diurnal and night hours throughout the summer months. For instance, May, June, July, and September showed temperature differences between the maximum and minimum temperatures by about 9 °C, whereas August and October were designated about 10 °C and 13 °C, respectively. This daily temperature variation required successful cooling strategies to maintain acceptable thermal comfort for occupants in such harsh locations.

The improvement in the indoor PCM room was studied in view of the AITR and TLLR in each case to specify the best window direction, as mentioned earlier.

3.2.1. Analysis of AITR under different window orientations

The AITR was determined for the PCM room with different orientations during the night period and compared with the one without NNV (oriented towards the east) to quantify the temperature reduction of the PCM room at each window orientation. It is worth mentioning that the AITR during the day was neglected since the NNV showed no influence on the indoor temperature during sunshine hours in locations of high ambient temperature throughout the day and nighttime [31]. Fig. 8 shows the AITR of the PCM room enhanced with NNV under all orientations compared with the non-ventilated PCM room during the night period.

Fig. 8 disclosed that the NNV through a single-sided window did not reduce the PCM room indoor temperature by more than 1 °C during May–September, regardless of window orientation. This is recognised due to the high night air temperature, which was insufficient to discharge heat from the PCM room considering the wind speed only. Besides, the figure displayed that the W and NW orientations are the best for NNV compared with the others during May–October, whereas the N and NE were the worst. The trend differed in October, where the S and SW orientations showed better AITR than the other orientations by more than 1.2 °C. Considering the wind speed and direction presented in Fig. 7, it could be observed that the wind direction is mostly from NW and W at the location under study. This is the main reason behind the best AITR at these orientations since the NNV depends mainly on the wind and buoyancy effect to ventilate the simulated room [51].

During hot months (May to September), the non-ventilated PCM room could be enhanced by an average AITR of about 0.51 °C 0.52 °C, 0.68 °C, 0.64 °C, 0.65 °C, 0.68 °C, 0.88 °C and 0.89 °C at the N, NE, E, SE, S, SW, W and NW directions, respectively. Besides, compared with the reference case (i.e., E orientation), only the W and NW orientations could improve the indoor temperature over the PCM room with an E-oriented window by 29.3% and 31.1%, respectively.

3.2.2. Analysis of TLLR under different window orientation

Fig. 9 presents the TLLR results of the PCM room under NNV and different orientations during the simulation period. It was revealed that the NNV had enhanced the room's thermal performance with a TLLR ranging between 9% and 17% during the investigated period. More precisely, The TLLR ranged between 8.9% and 10.2% in May, 12.4%–14.7% in June, 13.9%–15.8% in July, 13.3%–16.1% in August, 12.8%–14.6% in September and 16.5%–17.3% in October. It also was noted that the TLLR varied each month slightly with no specific trend of a particular orientation, except that the NE window orientation always achieved the lowest TLLR. Besides, the TLLR was lowest during May and highest in October, regardless of the window orientation. The highest summer months (i.e., June–September) showed a relatively similar TLLR trend, with a slight difference, in which July recorded the highest TLLR compared with the other months. This is because the difference between PCM room maximum and minimum temperatures during July is higher than in other months. This resulted from high air temperature at night in July with a slight effect for the NNV on the indoor temperature. It is worth mentioning that the wind speed was overlooked in this study since it was relatively similar in all months, reaching a maximum of 15 m/s, referring to Fig. 7.

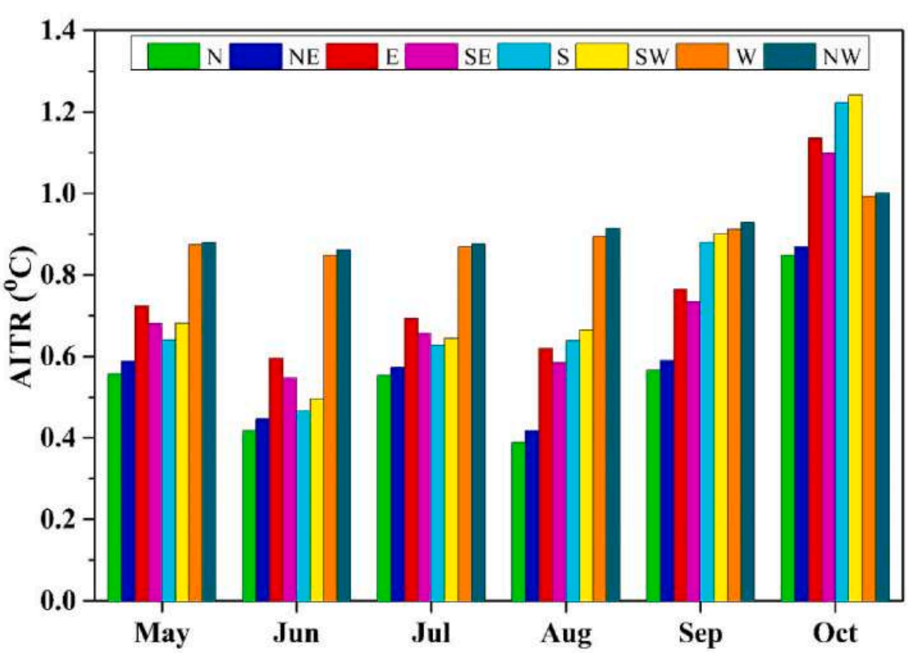

Fig. 8. AITR of PCM room with different window orientations.

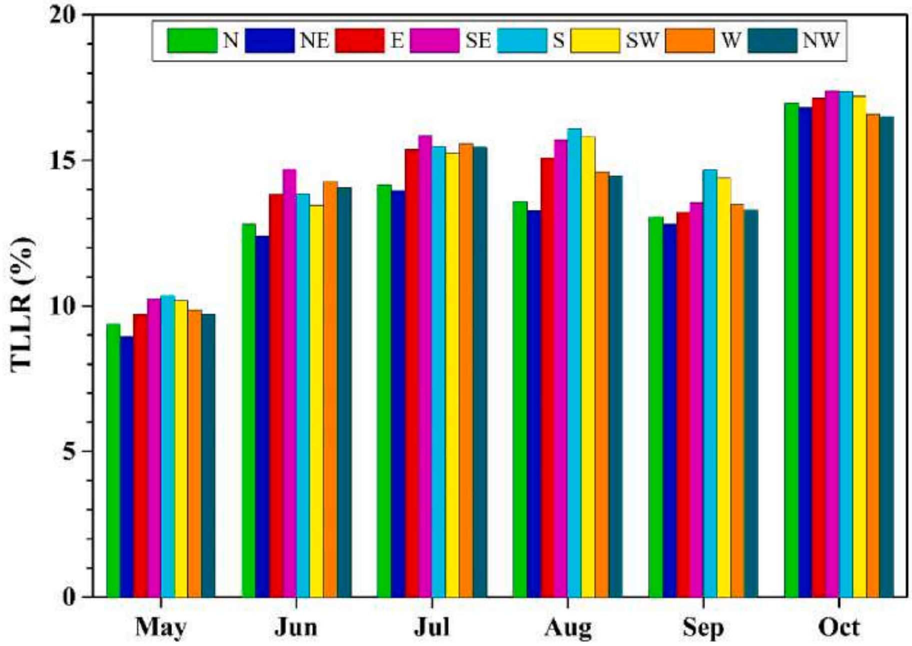

Fig. 9. Average TLLR of ventilated PCM room with different window orientations.

3.3. Effect of WWR on the indoor thermal enhancement

The influence of WWR on indoor thermal enhancement was analysed considering different WWRs, namely WWR10, WWR12, WWR14, WWR16, 18 WWR and 20 WWR, compared with the reference case of 8.75 WWR for the PCM room with NW orientation, the best case obtained in subsection 3.2. The effect of WWR on indoor thermal enhancement was analysed in view of the AITR and operative temperature reduction (OTR) in the PCM room-enhanced NNV at different WWRs compared with the PCM room with no ventilation.

Limited studies have studied the effect of window orientation on the indoor temperature improvement of a PCM-enhanced room/building. However, the selected orientations are mostly reasonable concerning the location under study and wind direction. Among others, Laasri et al. [52] numerically analysed the temperature fluctuation reduction of a light-weight square building integrated with PCM under Moroccan weather conditions. Considering the effect of window orientation, their study showed that the ventilation through the southern window has mostly enhanced the building indoor temperature compared with the N, E and W directions. Hu et al. [53] showed that the ventilation through S-oriented window could effectively improve the indoor thermal comfort and energy saving of PCM buildings in Denmark. In their experimental work, the authors revealed that the NV is necessary for precooling in the above location in which the indoor temperature was

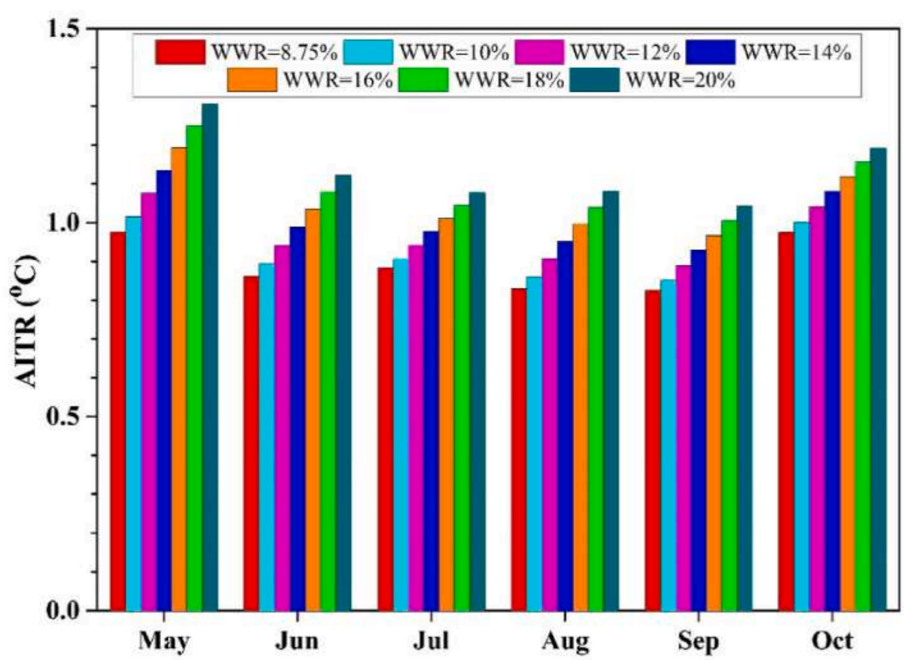

Fig. 10. AITR of PCM room with NW orientation and different WWRs.

decreased by 1.4 °C for 7 h in the PCM room compared with another reference room with ventilation only. Durakovic and Halilovic [54] experimentally investigated the effect of south-oriented window on the indoor thermal comfort of a solar wall containing PCM under Sarajevo, Bosnia weather conditions. The test results showed that the NV has improved the indoor thermal comfort during summer, maintaining the indoor space within the comfort range between 20 °C and 27 °C for 4 h–7 h daily, especially in the late afternoon and early evening.

3.3.1. Analysis of AITR of PCM room at different WWRs

The AITR of the PCM room-enhanced NNV with various WWRs is compared to the references PCM room with no ventilation (WWR = 8.75%). The calculation outcomes of the studied cases are displayed in Fig. 10.

Fig. 10 displayed that the AITR of the PCM room reduced as the WWR increased during the simulated period, indicating better thermal comfort. However, the influence of WWR was relatively similar during all months, except during May and October, which showed better AITR influenced by the colder nights. Considering all months, the AITR of PCM room was enhanced by 0.89 °C at WWR = 8.75%, 0.92 °C at WWR = 10%, 0.97 °C at WWR = 12%, 1.01 °C at WWR = 14%, 1.05 °C at WWR = 16%, 1.09 °C at WWR = 18% and 1.14 °C at WWR = 20% compared with the non-ventilated PCM room of WWR = 8.75%. These AITR values are equivalent to 3.2%, 8.4%, 13.5%, 18.1%, 22.9% and 27.5% at WWR of 10%, 12%, 14%, 16%, 18% and 20%, respectively, compared with the reference case of WWR = 8.75%.

The above results showed that applying NNV for 6 h at the best window orientation (NW) and WWR (20%) could decrease the PCM room temperature by a maximum of 1.14 °C over the case of a non-ventilated PCM room directed towards NW. This temperature reduction is too slight compared to the heat dissipated from the PCM at nighttime. Therefore, applying forced NV is suggested for such harsh weather locations considering the ventilation time and amount of ventilated air. Besides, an alternative cooling medium could be processed to expedite the PCM solidification phase.

3.3.2. Analysis of OTR in PCM room with different WWRs

The OTR results of the PCM room with different WWRs throughout the simulated months are presented in Fig. 11.

As designated in Fig. 11, the OTR of PCM was increased as the WWR increased, showing a notable difference each month. Considering all simulated months, the OTR ranged from 1.7% to 2.6%, 4.3%–6.8%, 6.9%–10.8%, 9.4%–14.8%, 11.8%–18.7% and 14.3%–22.5% at WWR of 10%, 12%, 14%, 16%, 18% and 20%, respectively compared with 8.75%. However, the OTR was slightly different in the simulated months at WWR = 10% and started to be sharper as the WWR increased to 20%.

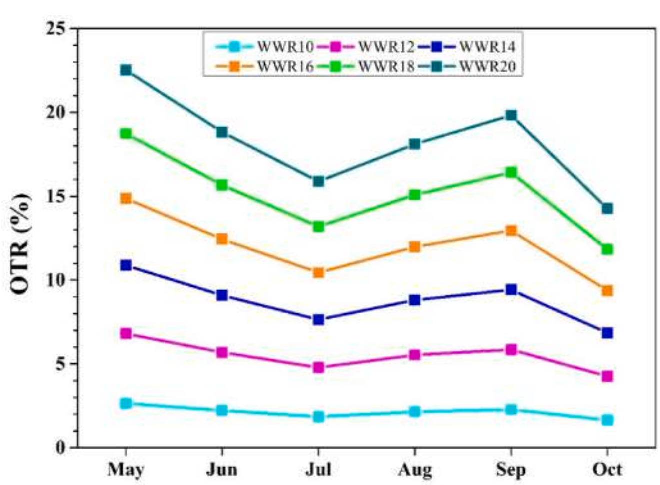

Fig. 11. OTR of PCM room with different WWRs.

The OTR was higher in May, followed by September, compared with the other months, whereas July showed lower OTR than August and Jun. The OTR in October was the lowest compared with all simulated months. The main reason behind this OTR fluctuation each month could be attributed to the varying night temperature each month, which was relatively low in May compared with the other hot months, like July. However, the situation differed in October, where the night temperature was too low, and increased WWR resulted in a slight increase in OTR compared with the original WWR.

Several literature studies have investigated the role of WWR in enhancing indoor comfort in different PCM building applications. For instance, Saber and Hajiah [55] numerically studied six different WWRs ranging from 10% to 70% with other aspects for buildings with PCM-drywalls under Kuwait City weather conditions. Considering the annual loads, the results showed that the WWR of 10% could lower the loads by 17.6%–20.5% and 4%–7.9% compared to the buildings with no drywall and PCM drywalls, respectively. Besides, the WWR of 40% showed the maximum annual total loads. The same PCM-dry wall application was investigated under different Spanish regions considering various WWRs, namely 10%, 20%, 30%, 40% and 60% [56]. The results generally showed improved indoor thermal comfort thanks to the PCM/WWR combination, in which the indoor temperature swing was smoothened by up to 60%, and the indoor thermal comfort period was extended by 1000–1600 h annually. Berardi and Soudian [57] investigated the effect of WWR = 80% combined with PCM high-rise apartments in Canada. The study outcomes showed that the peak indoor temperature was reduced by up to 6 °C thanks to the effect of high WWR and PCM integration into the walls and ceiling. Tunçbilek et al. [58] explored the effect of WWR = 25% for an office room with PCM walls in the Marmara region, Turkey. The study considered thermal comfort during workdays and off-days to show the contribution of ventilation through windows to thermal comfort. The proposed system has swinging of indoor temperature was reduced by 0.7 °C–1.4 °C.

4. Conclusion

This numerical study investigated the effect of natural night ventilation (NNV) to enhance the PCM room indoor temperature, considering the window orientation and the window-to-wall ratio (WWR). A numerical room model, validated with experimental data, was used to analyse several cases considering all window directions, and WWR varied from 8.75% to 20%. Several conclusions could be drawn from this study, such as:

- Wind direction significantly influences the window orientation when the PCM is combined passively with the building elements.
- The NNV has slightly improved the PCM room thermal performance, regardless of building orientation.
- The best performance was achieved in the Northwest direction in the studied location in which 1.2 °C diminished the PCM room indoor night temperature concerning the non-ventilated PCM room.
- Enlarged WWR significantly impacts the PCM room indoor temperature and maximises the effect of NNV. At the best room orientation (i.e., Northwest), increasing the WWR has diminished the PCM room average temperature by about 27.5% when enlarging WWR from 8.75% to 20%.
- The PCM room operative temperature reduction (OTR) increased as the WWR increased, and night temperature significantly influenced the monthly OTR. However, increased WWR has limited influence on the OTR of the PCM room in October, and window size has less impact during cold nights.

The study findings displayed limited effectiveness of NNV, attributable to high outdoor night temperatures. Therefore, using an alternate cooling medium is suggested for further research to tackle negative PCM behaviour during the heat discharging phase. Besides, cross ventilation could be a better option for such locations considering the reduced PCM amount incorporated, the size of windows, and their location.

CRediT authorship contribution statement

Qudama Al-Yasiri: Conceptualization, Methodology, Software, Formal analysis, Investigation, Writing – original draft, Writing – review & editing. **Mohammed Alktranee:** Conceptualization, Formal analysis, Investigation, Writing – review & editing. **Márta Szabó:** Conceptualization, Investigation, Writing – review & editing, Supervision, Funding acquisition. **Müslüm Arıcı:** Conceptualization, Software, Writing – review & editing.

Declaration of competing interest

The authors declare that they have no known competing financial interests or personal relationships that could have appeared to influence the work reported in this paper.

Acknowledgement

The first author appreciates the administrational and financial support of the Stipendium Hungaricum Scholarship Programme provided by Tempus Public Foundation and the Doctoral School of Mechanical Engineering, MATE-Szent István campus, Gödöllő, Hungary, during PhD studies.

References

[1] Z. Wang, Z. Yang, B. Zhang, H. Li, W. He, How does urbanisation affect energy consumption for central heating: historical analysis and future prospects, Energy Build. 255 (2022), 111631, https://doi.org/10.1016/j.enbuild.2021.111631.
[2] United Nations Environment Programme, Global Status Report for Buildings and Construction, 2022, 2022, https://www.unep.org/resources/publication/2022-global-status-report-buildings-and-construction.
[3] The intergovernmental Panel on climate change (IPCC), Climate Change 2022: Mitigation of Climate Change, 2022. https://www.ipcc.ch/report/ar6/wg3/.
[4] R.F. Rupp, N.G. Vásquez, R. Lamberts, A review of human thermal comfort in the built environment, Energy Build. 105 (2015) 178–205, https://doi.org/10.1016/j.enbuild.2015.07.047.
[5] A. Ciardiello, F. Rosso, J. Dell'Olmo, V. Ciancio, M. Ferrero, F. Salata, Multi-objective approach to the optimisation of shape and envelope in building energy design, Appl. Energy 280 (2020), 115984, https://doi.org/10.1016/j.apenergy.2020.115984.
[6] N. Soares, J. Bastos, L.D. Pereira, A. Soares, A.R. Amaral, E. Asadi, E. Rodrigues, F. B. Lamas, H. Monteiro, M.A.R. Lopes, A.R. Gaspar, A review on current advances in the energy and environmental performance of buildings towards a more sustainable built environment, Renew. Sustain. Energy Rev. 77 (2017) 845–860, https://doi.org/10.1016/j.rser.2017.04.027.
[7] L. Badarnah, Form follows environment: biomimetic approaches to building envelope design for environmental adaptation, Buildings 7 (2017) 40, https://doi.org/10.3390/buildings7020040.
[8] K. Haridass, N. N, S. Rajkumar, Experimental and numerical investigation on phase change material filled reinforced cement concrete roof slab for mitigating the heat transfer, Energy Sources, Part A Recover. Util. Environ. Eff 44 (2022) 3850–3865, https://doi.org/10.1080/15567036.2022.2068700.
[9] V.V. Kumar, Energy conservation of residential buildings in extreme climates with phase change material-aluminum radiation reflector cool roof, Energy Sources, Part A Recover. Util. Environ. Eff. 44 (2022) 9703–9715, https://doi.org/10.1080/15567036.2022.2136798.
[10] F. Hassan, F. Jamil, A. Hussain, H.M. Ali, M.M. Janjua, S. Khushnood, M. Farhan, K. Altaf, Z. Said, C. Li, Recent advancements in latent heat phase change materials and their applications for thermal energy storage and buildings: a state of the art review, Sustain. Energy Technol. Assessments 49 (2022), 101646, https://doi.org/10.1016/j.seta.2021.101646.
[11] K.A.R. Ismail, F.A.M. Lino, P.L.O. Machado, M. Teggar, M. Arıcı, T.A. Alves, M.P. R. Teles, New potential applications of phase change materials: a review, J. Energy Storage 53 (2022), 105202, https://doi.org/10.1016/j.est.2022.105202.
[12] M. Santamouris, K. Vasilakopoulou, Present and future energy consumption of buildings: challenges and opportunities towards decarbonisation, E-Prime - Adv. Electr. Eng. Electron. Energy. 1 (2021), 100002, https://doi.org/10.1016/j.prime.2021.100002.
[13] C. Piselli, M. Prabhakar, A. de Gracia, M. Saffari, A.L. Pisello, L.F. Cabeza, Optimal control of natural ventilation as passive cooling strategy for improving the energy performance of building envelope with PCM integration, Renew. Energy 162 (2020) 171–181, https://doi.org/10.1016/j.renene.2020.07.043.
[14] J. Lizana, M. de-Borja-Torrejon, A. Barrios-Padura, T. Auer, R. Chacartegui, Passive cooling through phase change materials in buildings. A critical study of implementation alternatives, Appl. Energy 254 (2019), 113658, https://doi.org/10.1016/j.apenergy.2019.113658.
[15] S. Alqaed, The effect of using phase change material in the natural ventilation duct of a building on temperature uniformity at different hours of the day, J. Build. Eng. 48 (2022), 103974, https://doi.org/10.1016/j.jobe.2021.103974.
[16] P. Arumugam, V. Ramalingam, P. Vellaichamy, Effective PCM, insulation, natural and/or night ventilation techniques to enhance the thermal performance of buildings located in various climates – a review, Energy Build. 258 (2022), 111840, https://doi.org/10.1016/j.enbuild.2022.111840.
[17] A. Mechouet, E.M. Oualim, T. Mouhib, Effect of mechanical ventilation on the improvement of the thermal performance of PCM-incorporated double external walls: a numerical investigation under different climatic conditions in Morocco, J. Energy Storage 38 (2021), 102495, https://doi.org/10.1016/j.est.2021.102495.
[18] H. Kitagawa, T. Asawa, T. Kubota, A.R. Trihamdani, Numerical simulation of radiant floor cooling systems using PCM for naturally ventilated buildings in a hot and humid climate, Build. Environ. 226 (2022), 109762, https://doi.org/10.1016/j.buildenv.2022.109762.
[19] C.G. Rangel, C.I. Rivera-Solorio, M. Gijón-Rivera, S. Mousavi, The effect on thermal comfort and heat transfer in naturally ventilated roofs with PCM in a semi-arid climate: an experimental research, Energy Build. 274 (2022), 112453, https://doi.org/10.1016/j.enbuild.2022.112453.
[20] J. Liu, Y. Liu, L. Yang, T. Liu, C. Zhang, H. Dong, Climatic and seasonal suitability of phase change materials coupled with night ventilation for office buildings in Western China, Renew. Energy 147 (2020) 356–373, https://doi.org/10.1016/j.renene.2019.08.069.
[21] J. Yu, K. Leng, H. Ye, X. Xu, Y. Luo, J. Wang, X. Yang, Q. Yang, W. Gang, Study on thermal insulation characteristics and optimised design of pipe-embedded ventilation roof with outer-layer shape-stabilised PCM in different climate zones, Renew. Energy 147 (2020) 1609–1622, https://doi.org/10.1016/j.renene.2019.09.115.
[22] Z. Luo, X. Liu, Q. Yang, Z. Qu, H. Xu, D. Xu, Numerical study on performance of porous brick roof using phase change material with night ventilation, Energy Build. 286 (2023), 112972, https://doi.org/10.1016/j.enbuild.2023.112972.
[23] A. Aamodt, A. Chaudhuri, H.B. Madessa, T.A. Vik, On the energy performance of micro-encapsulated phase change material enhanced spackling with night ventilation, Appl. Sci. 11 (2021) 1472, https://doi.org/10.3390/app11041472.
[24] M. Prabhakar, M. Saffari, A. de Gracia, L.F. Cabeza, Improving the energy efficiency of passive PCM system using controlled natural ventilation, Energy Build. 228 (2020), 110483, https://doi.org/10.1016/j.enbuild.2020.110483.
[25] M. Hou, X. Kong, H. Li, H. Yang, W. Chen, Experimental study on the thermal performance of composite phase change ventilated roof, J. Energy Storage 33 (2021), 102060, https://doi.org/10.1016/j.est.2020.102060.
[26] Z. Fan, Y. Zhao, Y. Shi, X. Liu, D. Jiang, Thermal performance evaluation of a novel building wall for light-weight building containing phase change materials and interlayer ventilation: an experimental study, Energy Build. 278 (2023), 112677, https://doi.org/10.1016/j.enbuild.2022.112677.
[27] U. Zavrl E, M. El Mankibi, M. Dovjak, U. Stritih, Experimental investigation of PCM system improved with nighttime ventilation for enhanced solidification, in: CLIMA 2022 14th REHVA HVAC World Congr, 2022, https://doi.org/10.34641/clima.2022.249. Rotterdam, The Netherlands.
[28] W. Ji, Y. Yuan, Y. Li, M. Yu, Wall-attached night ventilation combined with phase change material wallboard in hot summer: an experimental study on the thermal performance, J. Therm. Sci. 31 (2022) 318–331, https://doi.org/10.1007/s11630-022-1577-x.
[29] Y. Hu, R. Guo, P.K. Heiselberg, Performance and control strategy development of a PCM enhanced ventilated window system by a combined experimental and numerical study, Renew. Energy 155 (2020) 134–152, https://doi.org/10.1016/j.renene.2020.03.137.
[30] Y. Hu, P.K. Heiselberg, T.S. Larsen, Demand control strategies of a pcm enhanced ventilation system for residential buildings, Appl. Sci. 10 (2020) 4336, https://doi.org/10.3390/app10124336.
[31] Q. Al-Yasiri, M. Szabó, Phase change material coupled building envelope for thermal comfort and energy-saving: effect of natural night ventilation under hot climate, J. Clean. Prod. 365 (2022), 132839, https://doi.org/10.1016/j.jclepro.2022.132839.
[32] Q. Al-Yasiri, M. Szabó, Paraffin as a phase change material to improve building performance: an overview of applications and thermal conductivity enhancement techniques, Renew. Energy Environ. Sustain. 6 (2021) 38, https://doi.org/10.1051/rees/2021040.
[33] Q. Al-Yasiri, M. Szabó, Experimental evaluation of the optimal position of a macroencapsulated phase change material incorporated composite roof under hot climate conditions, Sustain. Energy Technol. Assessments 45 (2021), 101121, https://doi.org/10.1016/j.seta.2021.101121.
[34] Q. Al-Yasiri, M. Szabó, Case study on the optimal thickness of phase change material incorporated composite roof under hot climate conditions, Case Stud. Constr. Mater. 14 (2021), e00522, https://doi.org/10.1016/j.cscm.2021.e00522.
[35] Q. Al-Yasiri, M. Szabó, Thermal performance of concrete bricks based phase change material encapsulated by various aluminium containers: an experimental study under Iraqi hot climate conditions, J. Energy Storage 40 (2021), 102710, https://doi.org/10.1016/j.est.2021.102710.
[36] Ministry of Construction and Housing- Ministry of Planning,Thermal Insulation Blog (Iraqi Construction Blog), 2013. https://amanatbaghdad.gov.iq/amanarules/pict/مدونات/blog20-مدونة العزل الحراري.pdf.

[37] H.J. Akeiber, M.A. Wahid, H.M. Hussen, A.T. Mohammad, A newly composed paraffin encapsulated prototype roof structure for efficient thermal management in hot climate, Energy 104 (2016) 99–106, https://doi.org/10.1016/j.energy.2016.03.131.

[38] P.C. Tabares-Velasco, C. Christensen, M. Bianchi, Verification and validation of EnergyPlus phase change material model for opaque wall assemblies, Build. Environ. 54 (2012) 186–196, https://doi.org/10.1016/j.buildenv.2012.02.019.

[39] D. Abd El-Raheim, A. Mohamed, M. Fatouh, H. Abou-Ziyan, Comfort and economic aspects of phase change materials integrated with heavy-structure buildings in hot climates, Appl. Therm. Eng. 213 (2022), 118785, https://doi.org/10.1016/j.applthermaleng.2022.118785.

[40] R. Ye, H. Jiang, J. Wang, X. Yang, X. Shu, Fabrication and characteristics of eutectic hydrated salts/fumed silica composite as form-stable phase change materials for thermal energy storage, Sol. Energy Mater. Sol. Cells 238 (2022), 111584, https://doi.org/10.1016/j.solmat.2022.111584.

[41] D.A. El-Raheim, A. Mohamed, H. Abou-Ziyan, M. Fatouh, The essential properties governing the appropriate selection of phase change materials integrated into heavy structure buildings, Energy 266 (2023), 126515, https://doi.org/10.1016/j.energy.2022.126515.

[42] R.D. Beltrán, J. Martínez-Gómez, Analysis of phase change materials (PCM) for building wallboards based on the effect of environment, J. Build. Eng. 24 (2019), 100726, https://doi.org/10.1016/j.jobe.2019.02.018.

[43] R. and A.-C.E. American Society of Heating, ASHRAE Handbook-HVAC Systems and Equipment (IP Edition), ASHRAE, 2016, 2016.

[44] Z.X. Li, A.A.A.A. Al-Rashed, M. Rostamzadeh, R. Kalbasi, A. Shahsavar, M. Afrand, Heat transfer reduction in buildings by embedding phase change material in multi-layer walls: effects of repositioning, thermophysical properties and thickness of PCM, Energy Convers. Manag. 195 (2019) 43–56, https://doi.org/10.1016/j.enconman.2019.04.075.

[45] EnergyPlus^{TM} Version 22.1.0 Documentation: Engineering Reference, 2022. https://energyplus.net/assets/nrel_custom/pdfs/pdfs_v22.1.0/EngineeringReference.pdf.

[46] P.C. Tabares-Velasco, C. Christensen, M. Bianchi, C. Booten, Verification and Validation of EnergyPlus Conduction Finite Difference and Phase Change Material Models for Opaque Wall Assemblies, National Renewable Energy Lab.(NREL), Golden, CO (United States), 2012.

[47] V. Sharma, A.C. Rai, Performance assessment of residential building envelopes enhanced with phase change materials, Energy Build. 208 (2020), 109664, https://doi.org/10.1016/j.enbuild.2019.109664.

[48] E. Meng, H. Yu, B. Zhou, Study of the thermal behavior of the composite phase change material (PCM) room in summer and winter, Appl. Therm. Eng. 126 (2017) 212–225, https://doi.org/10.1016/j.applthermaleng.2017.07.110.

[49] ANSI/ASHRAE Standard 55-2010, Thermal environmental conditions for human occupancy, Encycl. Financ. (2010), https://doi.org/10.1007/0-387-26336-5_1680.

[50] Köppen Climate Classification, 2022. https://www.weatherbase.com/weather/weather-summary.php3?s=56604&cityname=Al+Amarah%2C+Maysan%2C+Iraq&units=.

[51] A. Aflaki, N. Mahyuddin, Z. Al-Cheikh Mahmoud, M.R. Baharum, A review on natural ventilation applications through building façade components and ventilation openings in tropical climates, Energy Build. 101 (2015) 153–162, https://doi.org/10.1016/j.enbuild.2015.04.033.

[52] I.A. Laasri, N. Es-sakali, A. Outzourhit, M.O. Mghazli, Evaluation of phase change materials for a light-weight building in Morocco: effect of building's volume, window orientation & infiltration, Energy Built Environ. (2023), https://doi.org/10.1016/j.enbenv.2023.06.013.

[53] Y. Hu, P.K. Heiselberg, R. Guo, Ventilation cooling/heating performance of a PCM enhanced ventilated window - an experimental study, Energy Build. 214 (2020), 109903, https://doi.org/10.1016/j.enbuild.2020.109903.

[54] B. Durakovic, M. Halilovic, Thermal performance analysis of PCM solar wall under variable natural conditions: an experimental study, Energy Sustain. Dev. 76 (2023), 101274, https://doi.org/10.1016/j.esd.2023.101274.

[55] H.H. Saber, A.E. Hajiah, 3D numerical modeling for assessing the energy performance of single-zone buildings with and without phase change materials, in: A. Bumajdad, W. Bouhamra, O.A. Alsayegh, H.A. Kamal, S.F. Alhajraf (Eds.), Gulf Conf. Sustain. Built Environ., Springer International Publishing, Cham, 2020, pp. 419–438.

[56] E. Rodriguez-Ubinas, B.A. Arranz, S.V. Sánchez, F.J.N. González, Influence of the use of PCM drywall and the fenestration in building retrofitting, Energy Build. 65 (2013) 464–476, https://doi.org/10.1016/j.enbuild.2013.06.023.

[57] U. Berardi, S. Soudian, Experimental investigation of latent heat thermal energy storage using PCMs with different melting temperatures for building retrofit, Energy Build. 185 (2019) 180–195, https://doi.org/10.1016/j.enbuild.2018.12.016.

[58] E. Tunçbilek, M. Arıcı, M. Krajčík, S. Nižetić, H. Karabay, Thermal performance based optimisation of an office wall containing PCM under intermittent cooling operation, Appl. Therm. Eng. 179 (2020), 115750, https://doi.org/10.1016/j.applthermaleng.2020.115750.